Peculiarities in formation of smoke aerosol dispersion structure at thermal decomposition of coniferous wood. 3. Afterburning of undecomposed fragments

R.F. Rakhimov, E.V. Makienko, and V.S. Kozlov

Institute of Atmospheric Optics,
Siberian Branch of the Russian Academy of Sciences, Tomsk

Received December 5, 2007

The microstructure of smokes from afterburning (at temperatures of ~ 700–800°C) of charcoal is analyzed. It is shown that the smoke particle size spectrum at afterburning of charcoal is noticeably different from smokes from thermal decomposition of resinous wood samples. The results of inversion of data of the polarization nephelometer have shown that, in spite of high temperature of decomposition and free oxygen access to the thermal decomposition chamber, the optical properties of the formed smoke are determined by finely dispersed particles with $r \approx 0.03$–0.35 μm and the complex refractive index $m \approx 1.590 - 0.011i$. The obtained estimations of the complex refractive index show a low content of the absorbing component (soot particles) as opposed to the usual smokes from burning. The volumetric concentration of medium-size particles in the range $0.35 < r < 0.7$ μm is negligibly small. The specificity of characteristics of optical and microphysical aerosols in this case is connected with a low content of complex organic compounds and resinous components in the structure of the burnt samples (charcoal).

Introduction

The smoke experiments in a Big Aerosol Chamber (BAC) performed within the framework of previous works[1–3] were developed in different directions. In particular, we considered peculiarities in formation of dispersion composition and the refractive index of smoke particles at variations of the mass of decomposed wood samples and the decomposition temperature. After completion of experiments with high temperature decomposition (T ~ 450–800°C) of coniferous wood with increased content of resinous compounds, there remained fragments only in the form of ashes in the thermal decomposition chamber (TDC) of the muffle furnace, which under slight mechanical impacts were easily powdered and kept in the composition of air flows for a long time.

In the experiments with low temperature pyrolysis (T ~ 200–300°C), the undecomposed pore coke fragments were extracted (charcoal) from the thermal decomposition chamber. Since small coke cubes of regular form were used in the first experiments, the remained fragments were close to the cubic form as well. Especially large amounts of such fragments were extracted from TDC in the experiments with a limited oxygen access at the low-temperature pyrolysis, i.e., in the mode of smoldering.

During a year and more, many experiments yielded a considerable amount of undecomposed fragments. The stability of the fragment shapes enabled us to use them in the experiment with a long-time repeated afterburning. Three loadings of the fragments as the initial material were required in the experiment, because of the limited TDC volume.

The results of spectronephelometric measurements and analysis of the dynamics of variation of parameters of smoke particle dispersion structure and refractive index, formed in afterburning of charcoals, are described in this paper. The methods of solution of inverse problem of aerosol light scattering were used for the optical data interpretation.

Discussion of results

A characteristic property of the high-temperature afterburning with the use of charcoals was the presence of slightly distinquishable visually flows of heated aerosol-gas mixture from the TDC to the BAC that predetermined the long process of filling the chamber with smoke aerosol. In particular, the homogeneity of filling and stability of optical signals was achieved only in 10 or 12 hours after the afterburning process onset. This can be seen from the time scan of optical signals (Fig. 1), recorded by the spectronephelometer at five scattering angles θ_k : 15; 45; 110; 135; and 165°; at nine wavelengths λ_i between 440 and 690 nm for two orthogonal polarization states of the incident radiation. In fact, we used 90 values of of directed light scattering coefficient $\beta_s(t, \theta_k, \lambda_i)$, $\text{km}^{-1} \cdot \text{sr}^{-1}$ for analysis of variations of smoke microstructure, which altogether composed a set of spectral-angular data at a particular moment. To solve the inverse problem, the initial data were formed according to the indicated time scans of signals with the use of analytical syncronization procedure.[3]

0235-6880/08/05 335-07 $02.00

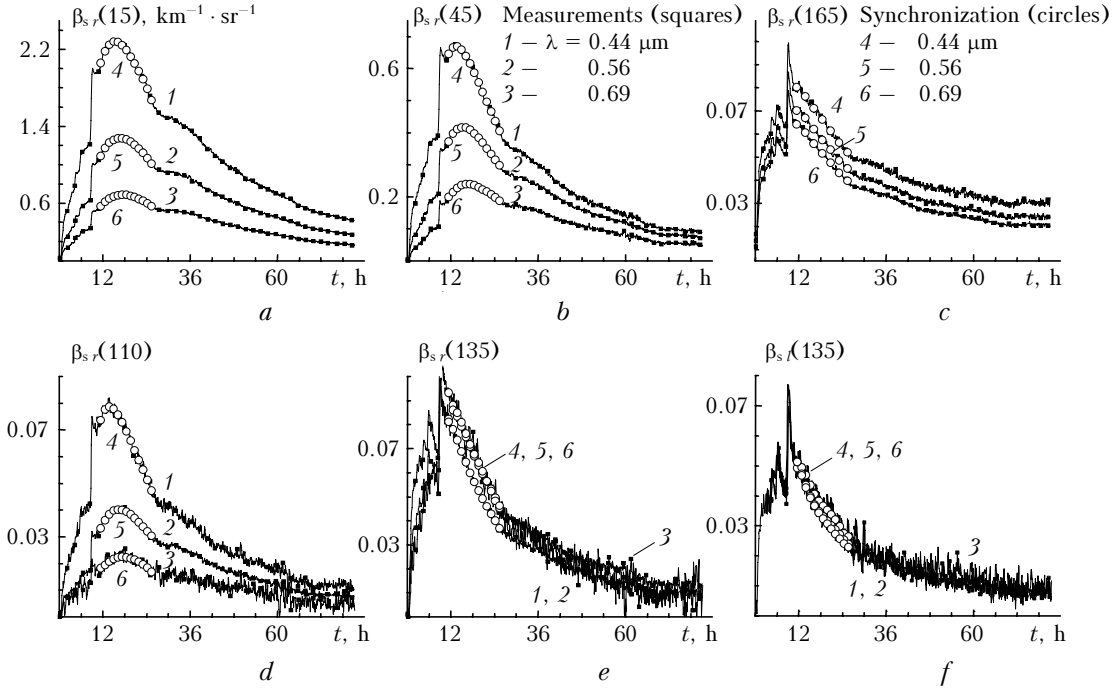

Fig. 1. Dynamics of variation of $\beta_s(t, \theta_k, \lambda_i)$, $km^{-1} \cdot sr^{-1}$ for $\lambda = 0.44$; 0.56; and 0.69 μm at charcoal decomposition in the burning mode: for the perpendicular component of polarization β_{sr} and scattering angles θ_k: 15 (*a*); 45 (*b*); 165 (*c*); 110 (*d*); 135° (*e*) and the parallel component β_{sl} for $\theta_k = 135°$ (*f*). The sample mass was 1250 g. Points of synchronization of measured data are shown by small circles.

The preanalysis of spectral-angular variation of $\beta_s(t, \theta_k, \lambda_i)$ by the magnitude and forward and back elongation of the scattering phase function, as well as the angular dependence of the degree of polarization of scattered radiation has shown that the smoke formed in the chamber differs by its characteristics from previously studied smokes[1] both by the dispersion composition and by the optical constants. Therefore, the results obtained within the framework of that experiment are discussed separately. The investigation methods and peculiarities of the experiment in the BAC were discussed earlier in detail.[3]

The afterburning of charcoals proceeds at high temperature $T \sim 700$°C in the burning mode (~11–12 hours). In contrast to previously considered pyrolysis smokes with limitation of air access (flameless pyrolysis),[1,2] the formed smoke remained for a long time in a limited closed volume, in spite of the closeness of the BAC walls. In this connection, the experiment length was increased up to 80 hours. The signals, recorded at the final stage (more than three days) signals, have made it possible to solve the inverse problem and to obtain the necessary in-depth information both on the index of refraction of smoke particles and on microstructural changes of the suspended dispersed mixture in spite of the increased relative measurement error.

The scanning of optical signals at the starting stage of the experiment shows (Figs. 1*a* and *b*) that when the chamber is filled with products of decomposition and optical signals increase, fluctuations of values of $\beta_s(t, \theta_k, \lambda_i)$ at $\theta_k \sim 15$ and 45° are small and steadily reproduce spatial inhomogeneities in filling the chamber with smoke particles. At the same time, at $\theta_k = 110$, 135, and 165° the relative magnitude of optical signal fluctuations increases simultaneously with the decrease of values of optical parameters at all considered wavelengths.

The pattern of the process is given in more detail in Fig. 2. A sharp increase in the optical signals in 9 hours after the start of the experiment is due to loading of the TDC with a new portion of the initial material.

Volume distributions of smoke particles reconstructed from the spectronephelometric data, measured during early 12 hours of the experiment, are shown in Fig. 3*a*.

A special attention must be given to instability of the distribution form (fluctuations in the content) of particles of finely dispersed fraction with $r < 0.16$ μm, which number density reaches $N \sim 10^6$ cm^{-3}. It is evident that when carrying out aerosol-gas mixture from the TDC to the BAC, the temperature contrasts arose between relatively cold air in the BAC and heated air flows from the TDC, which contain nanometer particles of anomalously high number density. This leads to their intensive coagulation. As a result of convection of inhomogeneously developed heated cells of aerosol–gas mixture, the cells complexly mix, causing spatial inhomogeneity in distribution of smoke particles. This is just the cause of the observed irregular variations of the spectral shape in the nanometer ($r < 100$ nm) size

interval. In 10 or 12 hours, the spatial distribution of small particles is gradually equalized and the retrieved spectra acquire a more stable character of variation (Fig. 3*b*). The stable and regular transformation of volume particle distribution in the final phase of the experiment is mainly determined by the aerosol runoff to the BAC walls.

Figure 4 shows the dynamics of variation of the retrieved values of the dispersed structure integral parameters: the number density N, the total cross section S, the integral volume V, and the effective radius of smoke particles r_{ef}. The values of the integral parameters (Table) are given in Fig. 4 at the unified scale through introduction of additional factors.

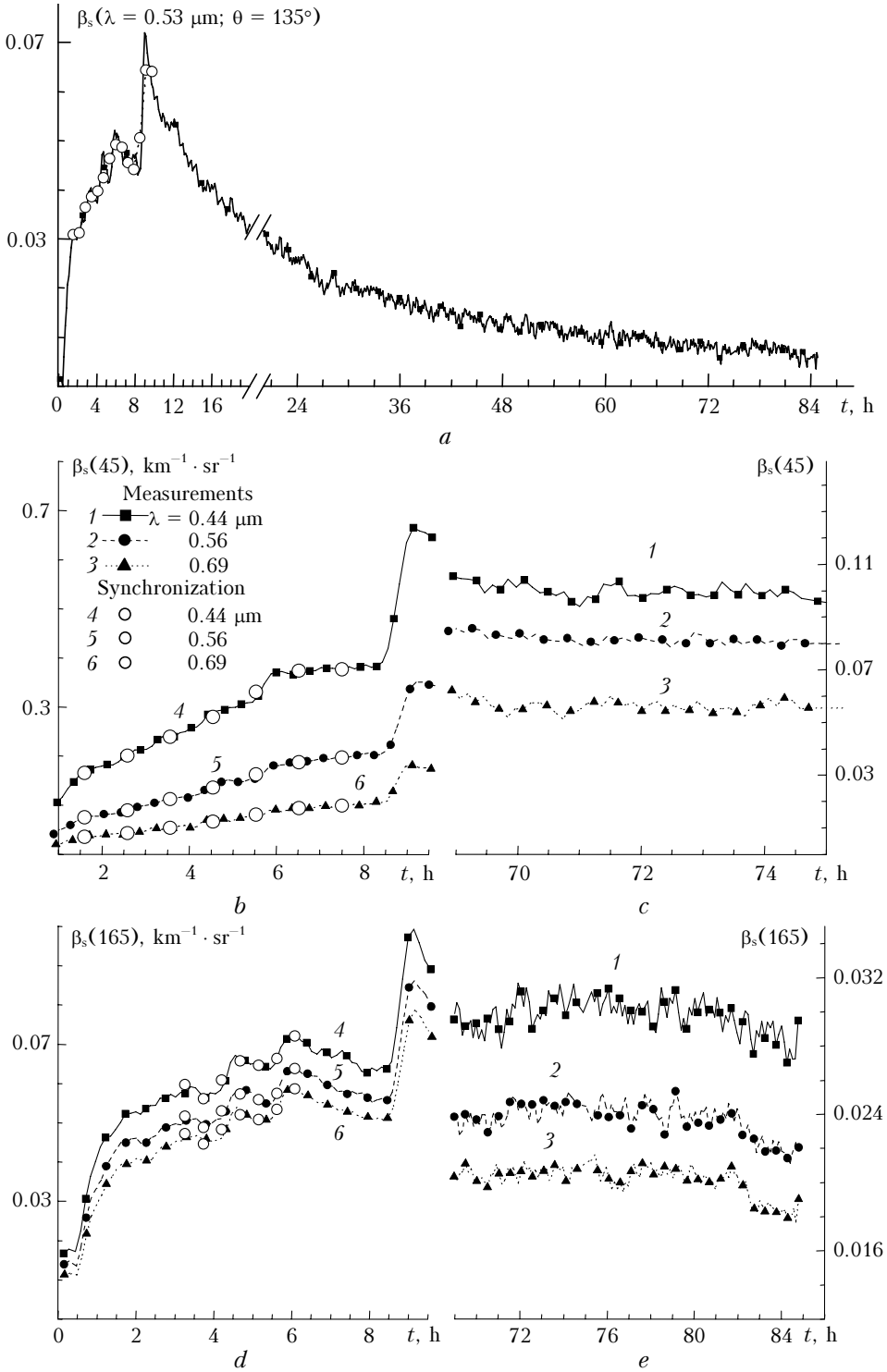

Fig. 2. The detailed time scan of variations of $\beta_s(t, \theta_k, \lambda_i)$ values: for $\theta_k = 135°$ and $\lambda = 0.53$ μm (*a*); at the initial stage (*b*, *c*) and at the final stage (*d*, *e*) of the experiment for $\lambda = 0.44$; 0.56; 0.69 μm and $\theta_k = 45$ (*b*, *c*) and 165° (*d*, *e*).

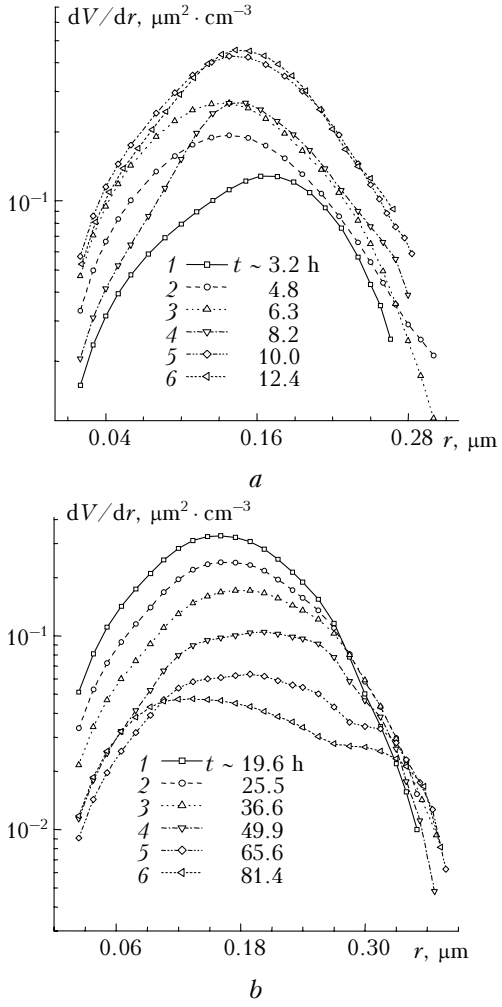

Fig. 3. The density of net volume size distribution of smoke particles at afterburning of the charcoals in the burning mode: at the initial stage of dispersed mixture formation (*a*); at the stage of relaxation and runoff to the BAC walls (*b*); $T \sim 700$°C; the sample mass $M \sim 1250$ g.

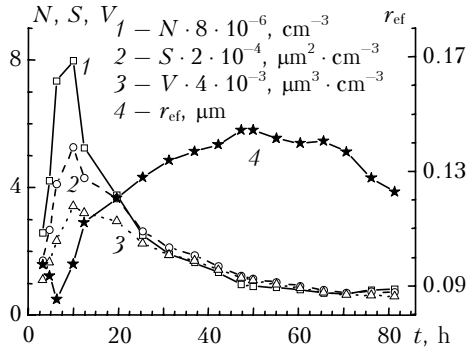

Fig. 4. The dynamics of variation of integral parameters of smoke microstructure in the process of charcoal afterburning without limitation of air access (burning). $T \sim 700$°C. $M \sim 1250$ g.

As is seen in Fig. 4, when afterburning charcoals, small aerosol with $r_{ef} \sim 0.07$–0.09 μm (curve *4*) is carried out from TDC to BAC. This is confirmed by the fact that as the maximum of smoke particle concentration in BAC is reached, the particle effective size reaches its minimum and a gradual increase of r_{ef} starts after 7–8 hours due to the coagulation process. The predominant influence of the process of coagulation growth of smoke particles in BAC continues about 50 hours and, as a result, the maximum value of effective size of smoke particles reaches ~ 0.145 μm. In the visible range of wavelengths, the smoke particles by the diffraction size fall within the so-called interval of Rayleigh particles. Then, the runoff of the largest particles to the chamber walls causes termination of the effective growth of particles, and the typical decrease of the share of large particles is set in the volume distribution (see Fig. 3*b*, curves *5* and *6*).

Table

t, h	*N*, 10^{-5} cm^{-3}	*S*, 10^{-4} μm^2 · cm^{-3}	*V*, 10^2 μm^3 · cm^{-3}	R_{ef}, μm
3.2	3.22	0.86	2.78	0.0974
4.8	5.26	1.33	4.14	0.0934
6.3	9.18	2.05	5.81	0.0852
10.0	9.97	2.63	8.55	0.0976
12.4	6.55	2.15	8.03	0.112
19.6	4.70	1.83	7.37	0.121
25.5	3.13	1.31	5.60	0.128
31.3	2.37	1.06	4.74	0.134
36.9	2.05	0.93	4.26	0.137
42.2	1.66	0.77	3.56	0.139
47.3	1.20	0.61	2.92	0.144
49.9	1.13	0.57	2.73	0.144
55.2	1.08	0.51	2.42	0.141
60.4	1.01	0.46	2.13	0.140
65.6	0.86	0.39	1.81	0.140
70.7	0.83	0.35	1.59	0.137
76.3	0.98	0.37	1.56	0.128
81.4	1.02	0.36	1.45	0.123

Despite rather high temperature and free access of oxygen to TDC (the afterburning proceeds in the burning mode), the estimates of the index of refraction gave very low values (for a given decomposition mode) of the imaginary part of the complex index of refraction: $m \sim 1.594$–$0.011i$.

Earlier it has been shown[1,2] that as the pyrolysis temperature increases, the share of moderate and coarse smoke aerosols decreases. The relative share of fine aerosols in this case increases. As the mass of samples grows, at the same temperature the density of smoke content increases, the smoke particle concentration grows, including the fine fraction. To combine the influence of the above factors in order to achieve the maximal filling of BAC with the fine component, the smoke experiment was performed with a high-temperature ($T \sim 830$°C) decomposition of a sample in the pyrolysis mode without the oxygen access. In the experiment, a large mass ($M \sim 1250$ g) of coniferous resinous wood was used.

Data of the spectronephelometric measurements show that sufficiently smooth time series of directed light scattering coefficients were obtained (Fig. 5).

From the solution of inverse problem of spectral-angular functions of variation of polarization components

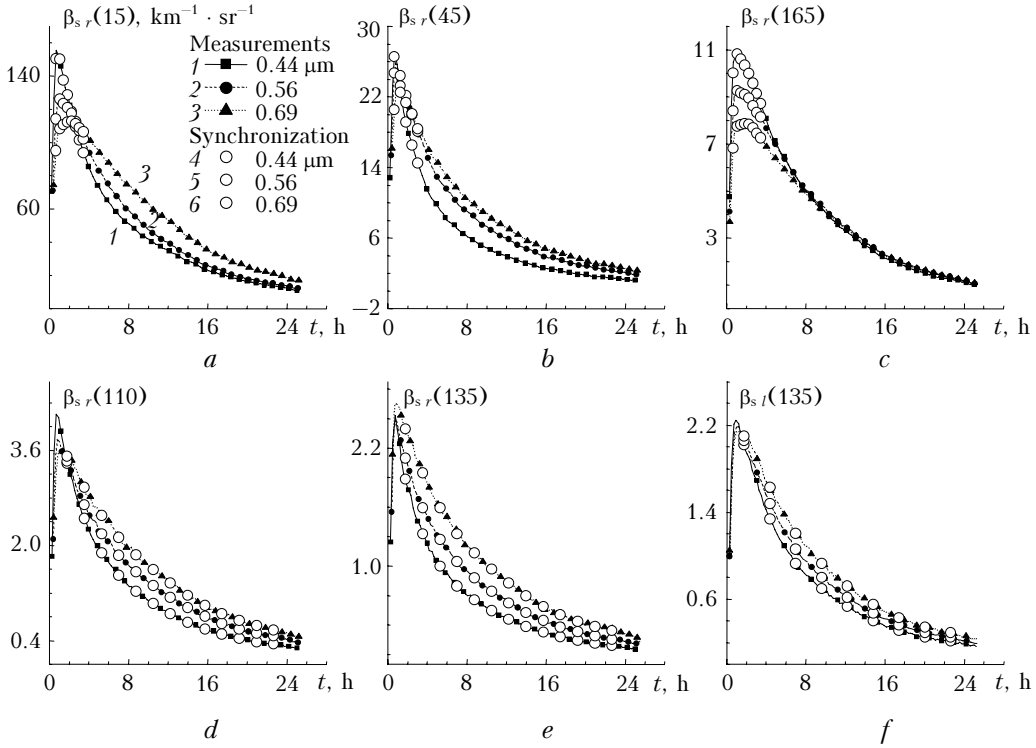

Fig. 5. Dynamics of variation of $\beta_s(t, \theta_k, \lambda_i)$ for $\lambda = 0.44$; 0.56; 0.69 μm at high-temperature pyrolysis of wood samples of $M \sim 1250$ g for a perpendicular component of polarization and $\theta_k = 15$ (*a*); 45 (*b*); 165 (*c*); 110 (*d*); 135° (*f*) and a parallel component at $\theta_k = 135°$ (*e*); points of synchronization of measured data are shown by circles.

of the directed light scattering coefficient (Fig. 5), the time transformation of the volume particle size distribution (Fig. 6) and the dynamics of variation of integral parameters of dispersed smoke structure (Fig. 7) were retrieved.

The initial size distribution of smoke particles (Fig. 6, curve *1*) is given for the moment ($t \sim 50$ min), that corresponds to the maximal values of $\beta_s(t, \theta_k, \lambda_i)$ (see Fig. 5) recorded in this experiment. Results of the solution of inverse problem, presented in Fig. 6, have shown that in spite of the fact that the wood sample mass was much larger (~1250 g) than in Ref. 1 (~800 g), at higher temperature of pyrolysis of resinous samples in the TDC ($T \sim 830$°C), the optical characteristics of a given smoke realization are determined by particles with radii no larger than 0.7 μm.

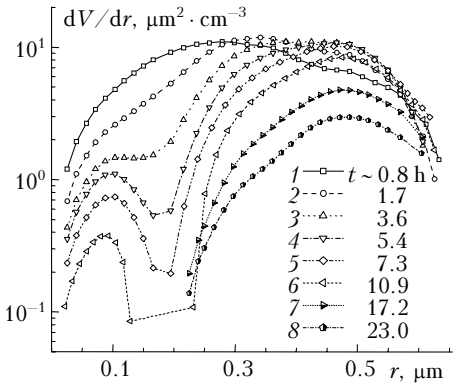

Fig. 6. Variations of size distribution density of net volume of smoke particles in the high-temperature ($T \sim 830$°C) pyrolysis without oxygen access of resinous (coniferous) wood of $M \sim 1250$ g.

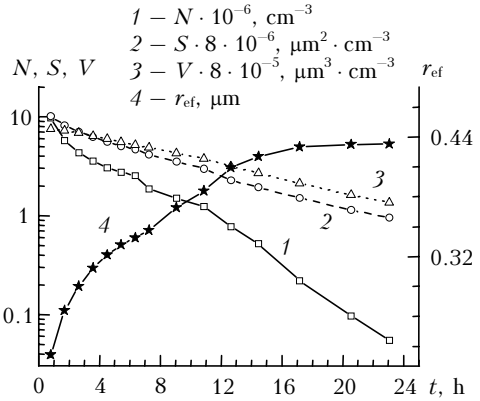

Fig. 7. Dynamics of variation of integral parameters of smoke microstructure in the high-temperature ($T \sim 830$°C) pyrolysis without oxygen access of resinous (coniferous) wood of $M \sim 1250$ g.

In contrast to the time dynamics of the smoke microstructure,[1,2] further development of the dispersed mixture shows that the run-off of the largest spectral particles (in this experiment, with $r > 0.4$ μm) is not so intensive. More essential changes in the spectrum were revealed in the size interval $r < 0.4$ μm (curves *1–4*, Fig. 6). During the indicated time interval, the

intensive run-off of small particles and fast increase of the effective size of particles of the dispersion mixture as a whole is observed (see curve *4* in Fig. 7). In 16 hours, the increase of the effective particle size begins to slow down and reaches the maximum, which retained during some time, although the optical smoke density continues to decrease as a result of particle runoff to the chamber walls (Fig. 5).

A special attention must be given to a fast decrease of the number density $N(t)$ as compared to a smoother time dependences of variation of the volume $V(t)$ and the summarized cross section $S(t)$. It is known that the number density of smoke particles is determined, first of all, by the behavior of the finely dispersed component, while the net cross section and especially the volume (in this experiment) depend on the processes regulating the development of dispersed composition in the moderate size range. All size fractions are involved in the process of coagulation of smoke particles in the large aerosol chamber. However, if in the process of coagulation there arise the decrease of the concentration of small particles and the increase of the concentration of large particles in the size range $r < 0.4$ μm, then in the moderate-dispersion range this process causes the accumulation of the aerosol matter (at the cost of small particles).

The dynamics of variation of curves *1–4* (Fig. 6) enables one to assume that in a given smoke realization, a high concentration of aerosol-forming gases (AFG) and nanometer particles with $r < 40$ nm is formed as a result of high-temperature decomposition of a sufficiently large (~60% of TDC volume) mass of a resinous sample. The optical contribution of these particles to the values of $\beta_s(t, \theta_k, \lambda_i)$ is at the level of instrumental noise, and therefore it cannot be found explicitly in spectra dV/dr by results of solution of the inverse problem. However, their presence manifests itself indirectly as the result of coagulation of nanometer particles with $r < 0.04$ μm, which leads to formation of rather narrow long-living mode within size range $0.04 < r < 0.025$ μm (curves *3–5*, Fig. 6).

Underline that the presence in the immediate vicinity of significant amount of moderately dispersed aerosols creates additional prerequisites for an effective cleaning of the chamber from the fine dispersed component of smoke, including nanometer particles with $r < 100$ nm. In fact, smoke particles of the moderately dispersed range form a supplementary surface to the chamber walls for runoff of products of thermal decomposition.

Simultaneously, the volume distribution of smoke particles in the BAC varied (Fig. 6) in the right side of the size spectrum $r > 0.25$ μm due to the gradual enlargement of moderately dispersed particles and the formation at the final stage of narrow fraction in the range of radii 0.3–0.7 μm. On the whole, the above-mentioned variations of microstructure of submicron smoke aerosol at a time interval of 15–16 hours lead to the increase of mean particle size up to $r_{ef} \sim 0.44$ μm. In the final phase of the process (17–24 hours) when the particle runoff to chamber walls makes a predominant impact on the variation of parameters of smoke microstructure, r_{ef} within the limits of calculation accuracy remains constant. The estimations of an effective value of the complex index of refraction m of smoke particles, obtained from the solution of inverse problem, at all stages of smoke growth were at the level $m \sim 1.62–0.007i$.

In conclusion, we compare the dynamics of transformation of the smoke particle size spectrum when burning of charcoals and at pyrolysis of resinous wood samples (Fig. 8). First of all, special attention must be given to essential differences of dispersed composition of smokes in the range from 0.28 to 0.70 μm. As it is seen, only finely dispersed particles are present in the composition of smokes of charcoal burning.

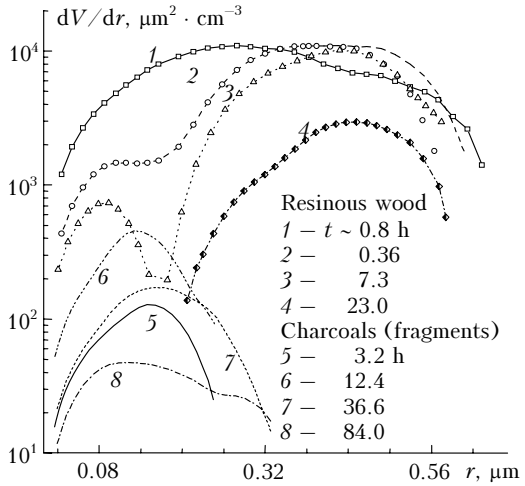

Fig. 8. Comparison of time transformation of the volume particle distribution in the pyrolysis without oxygen access ($T \sim 830$°C) of resinous wood of $M \sim 1250$ g (curves *1–4*) and the burning mode ($T \sim 830$°C) of charcoals of the same mass (curves *5–8*).

Besides, as it was mentioned earlier, the accumulation of finely dispersed component in the experiment with charcoal burning continued for a long time ($t \sim 12$ hours, curve *6* in Fig. 8), i.e., generation of finely dispersed particles takes pBACe also inside the BAC from the heated aerosol-forming gases carried out from the thermal decomposition chamber together with aerosol-gas mixture. When decomposing resinous wood in the pyrolysis mode, the maximum content of the finely dispersed constant is achieved already at the starting stage of the process $t \sim 50$ min (curve *1* in Fig. 8). In this case the finely dispersed smoke particles enter the BAC directly from the thermal decomposition chamber.

Conclusions

The smoke particle size spectrum and its time dynamics at charcoal burning and at thermal decomposition in the pyrolysis mode of resinous wood samples differ in qualitative and quantitative characteristics.

The experiment with afterburning of charcoals in the burning mode ($T \sim 700$°C) has shown that at reduced content of complex organic compounds including the resinous components (leaving the structure samples as a result of thermal decomposition and emission of products of pyrolysis in the preliminary experiments) the finely dispersed particles are mainly formed in the size range 0.03–0.35 μm. The estimates of the complex index of refraction of particles ($m \sim 1590–0.011i$), obtained from the solution of inverse problem, have revealed, in this case, an untypical low content of absorbing components as compared with smokes of burning of conventional wood samples.[4]

When reaching high concentrations of moderately dispersed ($0.3 < r < 0.75$ μm) aerosols during the process of high temperature ($T \sim 830$°C) pyrolysis of large mass (~1250 g) of resinous wood the prerequisites occur to the increase of intensity of run-off of a finely dispersed component.

The dynamics of variation of volume particle distribution enables us to assume that at high temperature pyrolysis of a large mass of resinous samples the high concentration of aerosol-forming gases and particles of size $r < 0.04$ μm is achieved. High concentration of these particles manifests itself as a result of the coagulation process at the size range $0.04 < r < 0.2$ μm in the form of long-living narrow mode.

Acknowledgements

This work was performed under the financial support of the Russian Foundation for Basic Research (Grant No. 06–05–64842).

References

1. R.F. Rakhimov, V.S. Kozlov, and E.V. Makienko, Atmos. Oceanic Opt. **21**, No. 3, 191–194 (2008).
2. R.F. Rakhimov, E.V. Makienko, and V.S. Kozlov, Atmos. Oceanic Opt, **21**, No. 4, 252–256 (2008).
3. R.F. Rakhimov, V.S. Kozlov, E.V. Makienko, M.V. Panchenko, and V.V. Shmargunov, Atmos. Oceanic Opt. **20**, No. 7, 561–567 (2007).
4. V.S. Kozlov, R.F. Rakhimov, V.P. Shmargunov, and E.V. Makienko, in: *Abstracts of Reports at the XIV Workshop "Siberian Aerosols,"* Tomsk (2007), p. 27.